Abstract

Iron (Fe) can limit phytoplankton productivity in approximately 40% of the global ocean, including high-nutrient, low-chlorophyll (HNLC) waters. However, there is little information available on the impact of CO_2-induced seawater acidification on natural phytoplankton assemblages in HNLC regions. We therefore conducted an on-deck experiment manipulating CO_2 and Fe using Fe-deficient Bering Sea waters during the summer of 2009. The concentrations of CO_2 in the incubation bottles were set at 380 and 600 ppm in the non-Fe-added (control) bottles and 180, 380, 600, and 1000 ppm in the Fe-added bottles. The phytoplankton assemblages were primarily composed of diatoms followed by haptophytes in all incubation bottles as estimated by pigment signatures throughout the 5 (controls) or 6 (Fe-added treatments) days incubation period. At the end of incubation, the relative contribution of diatoms to chlorophyll *a* biomass was significantly higher in the 380 ppm CO_2 treatment than in the 600 ppm treatment in the controls, whereas minimal changes were found in the Fe-added treatments. These results indicate that, under Fe-deficient conditions, the growth of diatoms could be negatively affected by the increase in CO_2 availability. To further support this finding, we estimated the expression and phylogeny of *rbcL* (which encodes the large subunit of RubisCO) mRNA in diatoms by quantitative reverse transcription PCR and clone library techniques, respectively. Interestingly, regardless of Fe availability, the expression of *rbcL* decreased in the high CO_2 treatments (600 and 1000 ppm). The present study suggests that the projected future increase in seawater pCO_2 could reduce the RubisCO transcription of diatoms, resulting in a decrease in primary productivity and a shift in the food web structure of the Bering Sea.

1. Introduction

The atmospheric CO_2 concentration has risen from a pre-industrial level of approximately 280 ppm to the present level of approximately 400 ppm (WMO, 2013). Since the industrial revolution, the ocean has absorbed about one-third of CO_2 emitted by human activity (Sabine et al., 2004). It is predicted that the atmospheric CO_2 concentration could reach more than 700 ppm by the end of the 21st century (Meehl et al, 2007), driving a surface seawater pH decrease of 0.3–0.4, the so-called “ocean

32 acidification" (Caldeira and Wickett, 2003). Such a rapid decrease in seawater pH has
33 most likely not occurred for at least millions of years in the earth's history (Pearson and
34 Palmer, 2000). Therefore, it has been suggested that these predicted changes in seawater
35 carbonate chemistry would have enormous impacts on the health and function of marine
36 organisms (Raven et al., 2005).

37 In the last decade, numerous studies have been performed to evaluate the impacts of
38 ocean acidification on marine phytoplankton. In laboratory incubation experiments
39 using individual species (a single strain), the response of phytoplankton to increased
40 CO_2 levels differed among phytoplankton species, possibly depending on their ability to
41 assimilate carbon (Riebesell and Tortell, 2011; Collins et al., 2014). In the natural
42 environment, these taxon-specific differences in CO_2 response can cause a shift in the
43 phytoplankton community composition (Engel et al., 2008; Meakin and Wyman, 2011;
44 Endo et al., 2013) and subsequent changes in ocean trophic structures and
45 biogeochemical cycles (Riebesell et al., 2007; Yoshimura et al., 2013). However, the
46 current understanding of the effects of elevated CO_2 on marine phytoplankton is still
47 insufficient at the community level.

48 In terms of physiology, CO_2 is fixed by the carboxylation enzyme ribulose
49 bisphosphate carboxylase/oxygenase (RubisCO) in the Calvin-Benson-Bassham (CBB)
50 cycle. In general, the half-saturation constant of the enzyme ranges between 20 and 70
51 μmol kg^{-1} CO_2 (Badger et al., 1998), whereas the ambient seawater CO_2 levels are
52 between 10 and 25 μmol kg^{-1}. Therefore, the present CO_2 concentration could be
53 insufficient to ensure effective RubisCO carboxylation. The progression of ocean
54 acidification could enhance photosynthetic carbon fixation in marine phytoplankton by
55 increasing CO_2 availability.

56 Recent advances in molecular biology techniques have enabled us to examine the
57 taxon-specific responses to environmental changes by quantifying functional gene
58 expression in natural phytoplankton assemblages. For example, John et al. (2007a)
59 developed a suite of quantitative reverse transcription PCR (qRT-PCR) assays to
60 quantify *rbcL* (gene encoding the large subunit of RubisCO) mRNA in *Synechococcus*,
61 haptophytes, and heterokonts including diatoms. John et al. (2007b) demonstrated a
62 strong negative correlation between diatom-specific *rbcL* mRNA abundance and

63 seawater pCO_2 in the Mississippi River plume, suggesting that diatoms were
64 responsible for the greatest drawdown in seawater pCO_2. In addition, positive
65 correlations between diatom-specific *rbcL* transcripts and light-saturated photosynthetic
66 rates (P_{max}) in seawater were reported (Corredor et al., 2004; John et al., 2007b). These
67 results suggest that *rbcL* expression in diatoms could be used to estimate the
68 photosynthetic carbon-fixation capacity of natural phytoplankton assemblages.
69 Therefore, quantification of clade-specific *rbcL* transcripts can be used to assess the
70 physiological photosynthetic responses of individual phytoplankton taxa to
71 environmental changes.

72 The oceanic Bering Sea investigated in this study is an HNLC region (Banse and
73 English, 1999), where low iron (Fe) availability limits phytoplankton growth and nitrate
74 utilization, so surface chlorophyll *a* (Chl *a*) concentrations usually remain low in the
75 summer (Suzuki et al., 2002). Despite the low phytoplankton biomass, the oceanic
76 domain has the greatest amount of total primary and secondary production in the Bering
77 Sea (Springer et al., 1996). Suzuki et al. (2002) reported that diatoms were the dominant
78 phytoplankton group in the oceanic regions of the Bering Sea in the summer. In
79 addition, Takahashi et al. (2002) showed that diatoms had the greatest contribution in
80 the sinking particles in the area. However, less is known about the combined effects of
81 ocean acidification and Fe enrichment on diatoms in such HNLC regions. In addition,
82 there are no reports on the effects of CO_2 and Fe availability on *rbcL* transcription of
83 natural diatom community in HNLC regions.

84 The purpose of this study is to clarify the responses of phytoplankton, especially
85 diatoms, to CO_2 enrichment under Fe-depleted and Fe-replete conditions in the Bering
86 Sea basin using on-deck bottle incubation. Recently, Sugie et al. (2013) reported
87 changes in phytoplankton biomass and nutrient stoichiometry in this experiment. They
88 showed that Chl *a* biomass decreased with increased CO_2 levels only in Fe-depleted
89 treatments, suggesting that Fe deficiency and increased CO_2 synergistically reduced the
90 growth of phytoplankton in the study area. In addition, Yoshimura et al. (2014)
91 demonstrated that the net production of particulate organic carbon (POC) and total
92 organic carbon (TOC) decreased under high CO_2 levels only in the Fe-limited
93 treatments, whereas those in the Fe-replete treatments were insignificantly different.

These studies suggest that the increase in CO_2 could have negative impacts on phytoplankton growth and/or organic-matter production especially under Fe-depleted conditions. However, the molecular mechanisms of photosynthetic carbon assimilation in phytoplankton assemblages were not mentioned in the previous studies. Therefore, in the present paper, we primarily focused on changes in *rbcL* transcription in diatoms with different CO_2 and/or Fe availability.

2. Materials and Methods

2.1 Experimental setup

The study was carried out aboard the R/V *Hakuho Maru* (JAMSTEC) during the KH-09-4 cruise in September 2009. The water samples for incubation were collected from 10 m depth at a station (53° 05' N, 177° 00' W) in the Bering Sea on 9 September with acid-cleaned Niskin-X bottles attached to a CTD-CMS system. A total of 300 L of seawater was poured into six 50 L polypropylene carboys through acid-clean silicon tubing with a 197 μm mesh Teflon net to remove large particles. Subsamples were taken from each carboy and poured into triplicate acid-cleaned 12 L polycarbonate bottles (total 18 bottles) for incubation. Initial samples were collected from each carboy. All sampling was carried out using a trace-metal clean technique to avoid any trace metal contamination. Prior to incubation, $FeCl_3$ solutions (5 nmol L^{-1} in final concentration) were added to 12 bottles in order to reduce Fe limitation for the phytoplankton communities. The CO_2 levels in the incubation bottles were manipulated by injecting CO_2 controlled dry air purchased from a commercial gas supply company (Nissan-Tanaka Co., Japan). The air mixtures were passed through 47 mm PTFE filters (0.2 μm pore size, Millipore) before being added to the incubation bottles. The detailed procedures for trace metal clean techniques were described in Yoshimura et al. (2013). The CO_2 concentrations were set at 380 and 600 ppm for the non-Fe-added (control) bottles (hereafter referred to as 'C-380' and 'C-600', respectively), and 180, 380, 600, and 1000 ppm for the Fe-added bottles (hereafter referred to as 'Fe-180', 'Fe-380', 'Fe-600', and 'Fe-1000', respectively). Incubation was performed on deck in temperature-controlled water-circulating tanks for 5 (controls) or 6 (Fe-added treatments) days at the in situ temperature (8.2°C) and 50% surface irradiance adjusted

by natural density screens. The sampling opportunities for each parameter are shown in Table S1.

2.2 Carbonate chemistry, nutrients, and Chl *a*

The detailed methodology and basic chemical and biological parameters were reported in Sugie et al. (2013). In brief, during the incubation experiment, samples were collected from the incubation bottles for dissolved inorganic carbon (DIC), total alkalinity (TA), nutrients, and Chl *a* determination. DIC and TA concentrations were measured with a total alkalinity analyzer using the potentiometric Gran plot method (Kimoto Electric) following Edmond (1970). The levels of pCO_2 and pH were calculated from the DIC and TA using the CO2SYS program (Lewis and Wallance, 1998). Concentrations of nitrate plus nitrite, nitrite, phosphate, and silicic acid were measured using a QuAATro-2 continuous-flow analyzer (Bran+Luebbe). The concentration of total dissolved Fe (TD-Fe) was determined by a flow-injection method with chemiluminescence detection (Obata et al., 1993). Chl *a* concentrations were determined with a Turner Design fluorometer (model 10-AU) with the non-acidification method (Welschmeyer, 1994).

2.3 HPLC and CHEMTAX analyses

Samples for high-performance liquid chromatography (HPLC) pigment analysis were collected on days 3 and 5 for the control treatments and on days 2, 4, and 6 for the Fe-added treatments. Water samples (400–1000 mL) were filtered onto GF/F filters under gentle vacuum (< 0.013 MPa) and stored in liquid nitrogen or a deep freezer (−80°C) until analysis. HPLC pigment analysis was performed following the method of Endo et al. (2013).

To estimate the temporal changes in phytoplankton community structure during incubation, the CHEMTAX program (MacKey et al., 1996) was used following Endo et al. (2013). Briefly, optimal initial ratios were obtained following the method of Latasa (2007). Matrix A was obtained from Suzuki et al. (2002) (Table S2), who examined phytoplankton community compositions in the Bering Sea. Matrices B, C, and D were also prepared to determine the optimal pigment/Chl *a* ratios (Table S2). The pigment

ratios of Matrices B and C were double and half the Matrix A ratio, respectively. For Matrix D, values of 0.75, 0.5, and 0.25 for dominant (rank in high pigment/Chl *a* ratio: 1–5), secondary (rank: 6–10), and minor (rank: 11–15) pigments, respectively, were multiplied by each pigment ratio of Matrix A. We averaged the successive convergent ratios after the 10 runs among the 4 matrices to identify the most promising initial pigment ratios. The calculated final pigment/Chl *a* ratios in both the control and Fe-added treatments (Table S3) were within the range of values reported in Mackey et al. (1996), Wright and van den Enden (2000), and Suzuki et al. (2002).

2.4 qPCR and qRT-PCR

Water samples for DNA and RNA analyses were collected on days 3 and 5 for the control treatments and on days 2, 4, and 6 for the Fe-added treatments. DNA samples (400–500 mL) were collected onto 25 mm, 0.2 μm pore size polycarbonate Nuclepore filters (Whatman) with gentle vacuum (< 0.013 MPa) and stored in liquid nitrogen or a deep freezer at −80°C until analysis. DNA extraction was performed following the method of Endo et al. (2013). Extracted DNA pellets were resuspended in 100 μL of 10 mM Tris-HCl buffer (pH 8.5).

For RNA analysis, seawater samples (400–500 mL) were filtered onto 25 mm, 0.2 μm pore size polycarbonate Nuclepore filters (Whatman) with gentle vacuum (< 0.013 MPa) and stored in 1.5 mL cryotubes previously filled with 0.2 g of muffled 0.1 mm glass beads and 600 μL RLT buffer (Qiagen) with 10 μL mL^{-1} β-mercaptoethanol (Sigma, St Louis, USA). RNA samples were stored in liquid nitrogen or a deep freezer at −80°C until analysis. Extraction and purification of RNA samples were performed using the RNeasy extraction kit (Qiagen) on a vacuum manifold with on-column DNA digestion using RNase-free DNase (Qiagen) according to the manufacturer's protocol. RNA was eluted using 50 μL of RNase-free H_2O. Total RNA was then reverse transcribed into complementary DNA (cDNA) using the PrimeScript™ RT regent Kit with gDNA Eraser (TaKaRa) following the manufacturer's specifications.

Following Smith et al. (2006), we used double-stranded DNA and single-stranded cDNA standards for DNA and cDNA quantification, respectively. Standard curves for *rbcL* DNA were generated from plasmid DNA (pUC18, TaKaRa) containing an artificial gene fragment (113 bp in size) of *rbcL* from the diatom *Thalassiosira*

188 *weissflogii* (CCMP1336). The plasmid DNA was linearized with *Hind*III (TaKaRa) and
189 quantified using a Thermo NanoDrop spectrophotometer (ND-1000). On the other hand,
190 to produce the cDNA standard, a PCR-amplified *rbcL* gene fragment of *T. weissflogii*
191 (CCMP1336) was inserted into a plasmid DNA (pCR2.1, Invitrogen). The plasmid
192 DNA was purified using the Plasmid maxi kit (Qiagen) and linearized with *Bam*HI
193 (TaKaRa), and in vitro transcription was performed using T7 RNA polymerase
194 (Invitrogen) for 2 hours at 37°C with Recombinant RNase Inhibitor (TaKaRa). To
195 eliminate DNA contamination, RNA was digested for 2 min at 42°C using gDNA
196 Eraser (TaKaRa). RNA was purified using an RNeasy column (Qiagen) following the
197 manufacturer's instructions and quantified with a Ribogreen RNA quantification kit
198 (Molecular Probes) using the manufacturer's standard. RNA was reverse transcribed
199 into cDNA using the PrimeScript^{TM} RT regent Kit with gDNA Eraser (TaKaRa).
200 Copy numbers of DNA and cDNA standards were calculated using the equation of
201 Smith et al. (2006), where the molecular mass of each nucleotide (or nucleotide pair) in
202 double- and single-stranded DNA is assumed to be 660 and 330 Da, respectively. Serial
203 dilutions of DNA and cDNA standards were prepared using sterilized Milli-Q water.
204 To amplify the *rbcL* gene and cDNA fragments from diatoms, the following specific
205 primer set designed by John et al. (2007a) was used.
206 Forward primer: 5'-GATGATGARAAYATTAACTC-3'
207 Reverse primer: 5'-TAWGAACCTTTWACTTCWCC-3'.
208 Real-time PCR amplification was performed using SYBR Premix Ex Taq II (Perfect
209 Real Time, TaKaRa) with primer concentrations of 0.4 μM each and a Thermal Cycler
210 Dice Real Time System (TP800, TaKaRa). Diluted nucleic acid standards were then
211 added to the PCR mixture. The thermal cycling conditions were 95°C for 60 s, then 40
212 cycles of 95°C 5 s and 52°C 60 s. The fluorescence intensity of the complex formed by
213 SYBR green and the double-stranded PCR product was continuously monitored from
214 cycle 1 to 40. Quantification was achieved by the second-derivative maximum method
215 (Luu-The et al., 2005), and the copy number for each sample was determined by the
216 standard curves generated by serial dilutions of the standards.
217
218 **2.5 Clone libraries**

219 Clone libraries of *rbcL* cDNA were constructed for the C-380 and C-600 samples on
220 day 3, and Fe-380 and Fe-600 samples on day 2. The cDNA samples were PCR
221 amplified with the diatom-specific primer set and thermal cycling condition described
222 above using the TaKaRa Ex Taq Hot Start Version (TaKaRa). Triplicate PCR products
223 were mixed and then purified with agarose gel electrophoresis and the PureLink Quick
224 Gel Extraction Kit (Invitrogen). Purified amplicons from cDNA samples were then
225 cloned into the pCR2.1 vector using the TOPO TA cloning kit (Invitrogen) following
226 the manufacturer's instructions. Thirty-five to 50 colonies were randomly picked from
227 each clone library. Correct cDNA insertions were identified by PCR amplification using
228 the M13 forward (5'-GTAAAACGACGGCCAG-3') and reverse
229 (5'-CAGGAAACAGCTATGA-3') primers flanking the cloning site. Plasmid DNA
230 containing the inserts was cycle-sequenced using the Big Dye Terminator v3.1 Kit
231 (Applied Biosystems) with the M13 forward primer. The cycle sequencing products
232 were cleaned by isopropanol precipitation. Sequencing was performed with a 3130
233 Genetic Analyzer (Life Technologies). The obtained sequences were compared with
234 *rbcL* sequences deposited in GenBank database (http://www.ncbi.nlm.nih.gov) using
235 the BLAST query engine. Our *rbcL* cDNA sequences were deposited in the DDBJ
236 database with the following accession numbers: AB985799–AB986033.
237
238 **2.6 Phylogenetic and diversity analyses**
239 The *rbcL* sequences obtained were assembled into operational taxonomic units
240 (OTUs) with > 95% sequence identity, and rarefaction curves were plotted for each
241 clone library with the software mothur v. 1.27 (Schloss et al., 2009). To estimate OTU
242 richness, chao1 index (Chao, 1984) values were calculated using the number of
243 singleton sequences obtained in this study. Genetic diversity was assessed based on the
244 Shannon-Wiener index (*H*', Shannon, 1948) and Simpson's index (1-*D*, Simpson, 1949).
245 The statistical significance of differences in the compositions of pairs of *rbcL* sequences
246 in the libraries was tested using LIBSHUFF (Singleton et al., 2001). The LIBSHUFF
247 program determined the integral form of the Cramer-von Mises statistic for each pair of
248 communities using 10,000 randomizations. Any two libraries were considered to be
249 significantly different from each other if the lower of the significance values generated

by the software was < 0.025 ($p < 0.05$).

2.7 Statistical analysis

Statistical analyses were performed with the program R (http://www.r-project.org). To assess the statistically significant differences between pCO_2 levels in the control treatments or between control and Fe treatments, Welch's *t*-test was used. Differences among pCO_2 levels in the Fe-added treatments were evaluated with Kruskal-Wallis one-way analysis of variance (ANOVA). Holm's test for multiple comparisons was used to identify the source of the variance. For all of the analyses, the confidence level was set at 95% ($p < 0.05$).

3 Results

3.1 Experimental conditions

The bubbling of CO_2-controlled air succeeded in creating significant gradients in pCO_2, pH, and DIC in the different CO_2 treatments except on day 4 in the Fe-added treatments, when those values did not significantly differ between Fe-380 and Fe-600 (Table 1; Fig. S1). The initial concentrations of nitrate, phosphate, and silicic acid were 18.06 ± 0.10, 1.47 ± 0.01, and 16.90 ± 0.12 μmol L^{-1}, respectively (Table 1). In the control bottles, these macronutrients remained until the end of the incubation in both CO_2 treatments except for silicic acid, which was almost depleted on day 5 in the C-380 treatment (Fig. S2). In the Fe-added bottles, macronutrients were depleted on days 4 or 5 in all CO_2 treatments (Fig. S2). The TD-Fe concentration was 1.35 nmol L^{-1} in the initial seawater, and it remained low throughout the experiment in the control treatments (Table 1). In the Fe-added treatments, the TD-Fe concentrations were 5.50 ± 0.10 nmol L^{-1} in the initial bottles and remained above 4 nmol L^{-1} until the end of incubation (Table 1). The initial Chl *a* concentration was 1.96 ± 0.14 μg L^{-1} (Table 1). In the control bottles, the Chl *a* concentration increased until the end of the incubation and reached 10.22 ± 0.89 μg L^{-1} in the C-380 and 6.28 ± 0.64 μg L^{-1} in the C-600 treatments (Fig. S3). In the Fe-added bottles, the Chl *a* concentration increased rapidly and reached the maximum on day 4 in the Fe-180 and Fe-380 treatments (27.51 ± 0.71 μg L^{-1} and 28.45 ± 3.40 μg L^{-1}, respectively) and on day 5 in the Fe-600 and Fe-1000

281 treatments (27.68 ± 0.44 μg L^{-1} and 27.32 ± 3.05 μg L^{-1}, respectively), then declined
282 toward the end of the incubation (Fig. S3).
283
284 **3.2 Phytoplankton pigments**
285 Throughout the experiment, the concentrations of fucoxanthin (Fuco), mainly a
286 biomarker for diatoms (Ondrusek et al., 1991; Suzuki et al., 2011), and
287 19'-hexanoyloxyfucoxanthin (19'-Hex), an indicator of haptophytes (Jeffrey and Wright,
288 1994), were relatively high among the phytoplankton pigments. In the control bottles,
289 the concentrations of Fuco and 19'-Hex increased over time and reached the maximum
290 values on day 5 in both the C-380 and C-600 treatments (Figs. 1a and c). After day 3,
291 the concentrations of Fuco and 19'-Hex were higher in the C-380 treatment than in the
292 C-600 treatment (day 5: Welch's *t*-test C-380 > C-600, $p < 0.05$), although no statistical
293 significance was assessed on day 3 because samples were collected from each single
294 bottle. In the Fe-added bottles, Fuco concentrations increased throughout the incubation
295 and reached the maximum values on day 6, whereas 19'-Hex concentrations decreased
296 after day 4 (Figs. 1b and d). The concentrations of Fuco were significantly different
297 among CO_2 treatments on day 6 (Kruskal-Wallis ANOVA, $p < 0.05$), although these
298 differences were not supported by multiple comparisons (Holm's test, $p > 0.05$).
299 Significant differences among CO_2 treatments were also found for the 19'-Hex
300 concentration on day 6 (Kruskal-Wallis ANOVA, $p < 0.05$), and the values in the
301 Fe-180 treatment was significantly higher than those in the Fe-1000 treatment (Holm's
302 test, $p < 0.05$).
303
304 **3.3 CHEMTAX outputs**
305 In the initial phytoplankton community, diatoms and haptophytes were the
306 predominant numbers of the phytoplankton groups (i.e., they contributed 45% and 17%
307 of the Chl *a* concentration, respectively). The initial contributions of chlorophytes,
308 cryptophytes, peridinin-containing dinoflagellates, pelagophytes, prasinophytes, and
309 cyanobacteria to the Chl *a* biomass were 10%, 9%, 8%, 5%, 4%, and 2%, respectively.
310 In the control bottles, the contributions of diatoms to the Chl *a* biomass increased with
311 time, and their contributions reached the maximum (70% at the C-380 and 60% at the

312 C-600 treatments) on day 5 (Fig. 2a). On day 5, the contribution of diatoms in the
313 C-380 treatment was significantly higher than that in the C-600 treatment (Welch's
314 *t*-test, $p < 0.05$). However, the contribution of haptophytes to the Chl *a* biomass was
315 higher in the C-600 treatment (21%) than in the C-380 treatment (14%) on day 5
316 (Welch's *t*-test, $p < 0.05$). Increases in the contributions of diatoms were also observed
317 in the Fe-added treatment, and the contributions reached the maximum (82–85%) on
318 day 4 in all CO_2 treatments (Fig. 2b). In terms of diatom contribution, a significant
319 difference among CO_2 treatments was not detected with Kruskal-Wallis ANOVA ($p >$
320 0.05) in the Fe-added bottles. The contributions of haptophytes to Chl *a* biomass did not
321 differ significantly among CO_2 levels in the Fe-added bottles (Kruskal-Wallis ANOVA,
322 $p > 0.05$).
323
324 **3.4 Expression of diatom *rbcL* gene**
325 A significant linear relationship between the Fuco concentration and the
326 diatom-specific *rbcL* gene copy number was found (regression analysis: $r^2 = 0.677$, $p <$
327 0.001, n = 28) in our experiment (Fig. 3). In the control bottles, the transcript abundance
328 normalized to gene abundance (i.e., cDNA/DNA) of the diatom-specific *rbcL* gene
329 fragment for the C-380 treatment was significantly higher than that of the C-600
330 treatment on day 3 (Fig. 4; Welch's *t*-test, $p < 0.05$). In the Fe-added bottles, the
331 cDNA/DNA ratio of the diatom *rbcL* fragment in the lower CO_2 treatments (Fe-180 and
332 Fe-380) was higher than that in the Fe-600 treatment on day 2 (Fig. 4; Holm's test, $p <$
333 0.05).
334
335 **3.5 Clone libraries of diatom *rbcL* cDNA**
336 Rarefaction curves were plotted for the *rbcL* cDNA libraries (Fig. 5). In terms of
337 unique taxa, the highest number of OTUs was found in the C-380 treatment (Table 2).
338 The highest chao1value was found in the C-600 treatment, whereas the lowest value
339 was found in the Fe-600 treatment. Shannon-Wiener and Simpson diversity indices
340 revealed that the cDNA libraries in the 380 ppm CO_2 bottles were more diverse than
341 those in the 600 ppm CO_2 bottles in both the control and Fe-added treatments, although
342 the values were not statistically significant between CO_2 treatments (*t*-test, $p > 0.05$)

343 (Table 2).

344 All sequences obtained from the cDNA libraries were more than 95% similar to
345 sequences deposited in the GenBank. These sequences could be classified into the
346 following 11 phylogenetic groups: Chaetocerotaceae, Coscinodiscaceae,
347 Cymatosiraceae, Stephanodiscaceae, Thalassiosiraceae, unidentified centrics,
348 Bacillariaceae, Naviculaceae, Fragillariaceae, unidentified pennates, and other
349 eukaryotes by comparison with known *rbcL* sequences from GenBank. Sequences that
350 could not classified into a specific diatom family (e.g., closely related to two or more
351 diatom families with same similarity score) were assigned as unidentified centrics or
352 unidentified pennates. Other eukaryotes consisted of haptophytes, pelagophytes,
353 dictyochophytes, dinoflagellates, and diatoms which could be assigned to centrics and
354 pennates. For all of the cDNA libraries, more than 88% of *rbcL* sequences were most
355 closely affiliated with those of cultured diatoms. In the initial cDNA library, the most
356 abundant sequences were closely affiliated with the diatom family Bacillariaceae (46%),
357 followed by other eukaryotes and Cymatosiraceae (17% and 14%, respectively) (Fig. 6).
358 The contributions of other diatom groups were less than 6% in the initial clone library.
359 In the control bottles, the contributions of Coscinodiscaseae increased to 12–14%,
360 whereas those of Cymatosiraceae decreased to 4%. In the Fe-added bottles, the
361 contributions of Chaetocerotaceae and unidentified centrics to the total increased to
362 more than 8% and 20%, respectively. In contrast, the contributions of Bacillariaceae
363 decreased below 24% in both the Fe-380 and Fe-600 treatments.

364 Statistic analysis using LIBSHUFF revealed that the cDNA libraries in the control
365 treatments were not significantly different from the initial sample regardless of the CO_2
366 level, whereas those in the Fe-added bottles differed significantly from the initial
367 assemblage (LIBSHUFF, $p < 0.05$) (Table 3). No significant difference in the cDNA
368 library was found between C-380 and C-600 treatments in the control bottles
369 (LIBSHUFF, $p > 0.05$). However, a significant difference between the Fe-380 and
370 Fe-600 treatments was detected in the Fe-added bottles (LIBSHUFF, $p < 0.05$). In
371 addition, cDNA libraries in the Fe-added bottles differed significantly from those of the
372 control bottles in both the Fe-380 and Fe-600 treatments (LIBSHUFF, $p < 0.05$).
373

4 Discussion

4.1 Changes in phytoplankton community structure during incubation

Our CHEMTAX analysis suggested that the diatoms were the principal contributors to the Chl *a* biomass in the initial phytoplankton community, followed by haptophytes (Fig. 2). The results were consistent with those reported by Suzuki et al. (2002), who examined the community structure in the Bering Sea during early summer of 1999. These results suggest that diatoms and haptophytes are ecologically important phytoplankton groups in the study area during the summer. Compared with previous reports in the area (Suzuki et al., 2002; Yoshimura et al., 2013), a relatively high initial Chl *a* concentration was observed in our experiment, possibly due to an intrusion of the coastal seawater mass from the Aleutian trenches (Sugie et al., 2013). However, the Fe infusion induced significant increases in Chl *a* biomass and concomitant rapid drawdowns of macronutrients in our incubation bottles (Fig. S2). This indicates that the seawater used for the incubation was Fe-limited for phytoplankton assemblages. Our HPLC and CHEMTAX results suggested that the increase in phytoplankton biomass was mainly due to an increase in diatoms (Figs. 1b and 2b).

We found that the growth of Fuco was less in the high CO_2 bottles in the control treatments (Fig. 1a), suggesting that the elevated CO_2 levels could have a negative impact on the diatom biomass in the study area. Negative effects on diatoms induced by an increase in CO_2 availability were also reported in field incubation experiments conducted in the Bering Sea and the Okhotsk Sea (Hare et al., 2007 and Yoshimura et al., 2010, respectively). However, such trends have rarely been observed in other regions of the world's oceans (e.g., Tortell et al., 2002; Kim et al., 2006; Feng et al., 2009; Hoppe et al., 2013; Endo et al., 2013). Therefore, the responses of phytoplankton assemblages to ocean acidification can differ among geographic locations due to the differences in the biogeography of phytoplankton and/or environmental conditions.

One possible cause of the geographic specificity in the open Bering Sea is the differences in the species composition of diatoms. Our microscope data showed that centric diatoms such as Chaetocerataceae and Rhizosoreniaceae were predominant at the beginning of the incubation in terms of carbon biomass, and the coastal diatom species *Chaetoceros* spp. became predominant in all incubation bottles after day 2 (Sugie et al., 2013). Therefore, the relative decrease in Fuco biomass with increased

406 CO_2 levels might be partially explained by the decrease in *Chaetoceros* spp. A previous
407 field incubation experiment conducted in the Bering Sea also showed that the carbon
408 biomass of the *Chaetoceros* spp. decreased at higher CO_2 levels (600–960 μatm CO_2),
409 although it increased at 1190 μatm CO_2 (Yoshimura et al., 2013). However, Tortell et al.
410 (2008) demonstrated that relative abundance of *Chaetoceros* spp. increased under
411 elevated CO_2 levels in the Ross Sea. In the previous laboratory culture experiments, the
412 effects of increased CO_2 on the growth and/or photosynthesis of *Chaetoceros* spp. were
413 also inconsistent. For example, Ihnken et al. (2011) demonstrated that the growth of
414 diatom *Chaetoceros muelleri* decreased with elevated CO_2 (decreased pH) levels
415 although their photosynthetic capacity increased. In contrast, Trimborn et al. (2013)
416 showed a significant increase in the growth rate of *Chaetoceros debilis* under high CO_2
417 condition. In addition, no CO_2-related change in the growth and photosynthetic
418 physiology of *Chaetoceros brevis* was found (Boelen et al., 2011). These results suggest
419 that the responses to elevated CO_2 differ among *Chaetoceros* species.
420 The concentrations of 19'-Hex were significantly lower in the C-600 treatment than
421 those in the C-380 treatment (Fig. 1c), suggesting that the ocean acidification could
422 induce negative effects not only on the biomass of diatoms, but also on that of
423 haptophytes in the study area. Similar results were obtained from the previous field
424 studies in other regions (e.g., Feng et al., 2010; Endo et al., 2013). One possible factor
425 underlying these decreases is that the reduced carbonate-saturation states under high
426 CO_2 conditions. The energetic cost of calcification in coccolithophores will increase
427 with a decrease in pH (Mackinder et al., 2010). Therefore, additional energy might be
428 needed for cell growth in seawater with high CO_2 levels. In addition, non-calcifying
429 haptophytes such as *Phaeocystis* spp. often dominate among haptophytes in the natural
430 phytoplankton community (Schoemann et al., 2005), although the effects of ocean
431 acidification on them are still not well understood. Therefore, additional study using a
432 wide range of haptophyte species would be required for a detailed understanding of the
433 responses of the haptophyte community to CO_2-induced ocean acidification.
434 Our CHEMTAX outputs showed that the relative contributions of diatoms decreased
435 with increased CO_2 levels, whereas the contributions of haptophytes increased in both
436 the control and Fe-added bottles (Fig. 2). This indicates that the negative impacts of
437 increased CO_2 on diatoms were greater than those on haptophytes and other

phytoplankton groups. Another possibility is that the competitions between diatoms and other phytoplankton taxa could occur. For example, diatoms could become less competitive when silicic acid is exhausted, because Si-depletion significantly depressed the growth and could induce their cell death (Harrison et al., 1977; Jiang et al. 2014). However, concentrations of silicic acid were not significantly different among CO_2 levels in the Fe-added treatments (Fig. S2f). Moreover, in the control treatments, silicic acid was almost depleted in the low CO_2 treatment after day 5 but not in the high CO_2 treatment (Fig. S2e). These results suggest that availability of silicic acid little affected the decreases in relative diatom contribution to Chl *a* biomass. Larger diatoms can contribute to efficient transfer of energy and organic compounds to higher trophic levels because they would create a shorter food chain compared with nano- and pico-sized phytoplankton (Michaels and Silver, 1988). Because diatoms form a large part of phytoplankton biomass in the Bering Sea basin (Suzuki et al., 2002; Takahashi et al., 2002), the decrease in the relative contribution of diatoms with increasing CO_2 could reduce the energy transferred from the primary producers to the higher trophic levels.

The decreases in Fuco growth and relative contribution of diatoms were larger in the control bottles than those in the Fe-added treatments (Figs. 1 and 2), suggesting that the negative effect of CO_2 enrichment was greater in the Fe-limited conditions. These results are consistent with Sugie et al. (2013) and Yoshimura et al. (2014), who observed significant decreases in diatom carbon biomass and particulate organic carbon (POC) production under high CO_2 levels in the control treatments, whereas those were insignificantly changed in the Fe-added treatments. Sugie et al. (2013) indicated that the Fe limitations for phytoplankton in the control bottles were enhanced at high CO_2 levels, likely due to the reduction of Fe bioavailability as reported in Shi et al. (2010). The combined effects of CO_2 and Fe availability were also tested in a diatom-dominated phytoplankton community in the Southern Ocean (Hoppe et al., 2013). In their study, net primary productivity in seawater decreased with increased pCO_2 levels in the Fe-depleted treatments but not in the Fe-enriched treatments. These studies indicate that an interactive effect of CO_2 enrichment and Fe limitation could occur in the diatom-dominated natural phytoplankton assemblages in the HNLC region.

4.2 *rbcL* expression in diatom

A significant correlation between diatom *rbcL* copies per liter and Fuco concentration was found in this study (Fig. 3), suggesting the usefulness of the *rbcL* gene fragment as a proxy for diatoms. In addition, the cDNA sequences obtained from cloning were dominated by the diatom-derived *rbcL* gene (Fig. 6). These results indicate that the *rbcL* primers used successfully and selectively amplified the *rbcL* gene of diatoms. Suzuki et al. (2011) showed that Fuco concentration significantly correlated with diatom carbon biomass in the subarctic Pacific. Furthermore, Matsuda et al. (2011) showed that the number of *rbcL* gene per cell varies among diatom species, and it was positively correlated with cell size. Therefore, we concluded that the *rbcL* gene could serve as a potential molecular marker for diatom biomass.

The transcription of the diatom-specific *rbcL* gene decreased with elevated CO_2 levels in both the control and Fe-added treatments (Fig. 4). Because RubisCO expression is primarily controlled at the transcriptional level in the natural phytoplankton community (Xu and Tabita, 1996; Wawrik et al., 2002), our results suggest that increased CO_2 levels could reduce the amount of RubisCO in diatoms. It should be noted that significant decreases in *rbcL* expression with increased CO_2 levels were observed on days 2 or 3, when macronutrients still remained (Fig. S2). This indicates that the downregulation of *rbcL* expression in diatoms was probably caused by the increase in CO_2 availability. It has been shown that some land plants can increase their nitrogen utilization efficiency under elevated CO_2 levels by reducing the investment of nitrogen in RubisCO (Curtis et al., 1989; Makino et al., 2003). Losh et al. (2012; 2013) also demonstrated a decreased RubisCO contribution to the total protein in the California Current phytoplankton community with an increase in CO_2 level. Because a decrease in the expression of RubisCO can result in a reduction of the potential capacity for carbon fixation in the natural environment (John et al., 2007b), our results indicate that an increase in CO_2 levels could have a negative impact on photosynthetic carbon fixation for diatoms in the study area. Recently, Gontero and Salvucci (2014) pointed out that RubisCO activase plays a key role in the modification of RubisCO activity, and consequently in the capacity of carbon fixation, although the occurrence of RubisCO activase in diatoms is not well understood. Further studies must be needed for better understanding of the impacts of elevated CO_2 on photosynthetic

physiology in diatoms.

The negative effects of increasing CO_2 on diatom biomass were not severe in the Fe-added bottles relative to Fe-limited control bottles (Figs. 1a and b), whereas *rbcL* transcription decreased with increased CO_2 regardless of Fe availability (Fig. 4). This suggests that the diatoms could overcome the decrease in RubisCO activity in the Fe-added treatments. According to our cloning data (Fig. 6), a shift in phylogenetic composition of the diatoms actively transcribed *rbcL* was observed in the Fe-added bottles. In addition, F_v/F_m values increased significantly with Fe enrichment in our incubation experiments (Sugie et al., 2013), indicating an increase in the photochemical quantum efficiency of photosystem II for the diatoms. Therefore, the photosystem II activity might compensate for the decrease in RubisCO expression under Fe-replete conditions.

It is generally recognized that phytoplankton autonomously regulate the transcription of the *rbcL* gene in response to environmental conditions such as light and nutrient availability (Pichard et al., 1996; Granum et al., 2009; John et al., 2010). However, the mechanisms controlling the transcription of RubisCO operon in diatoms are largely unknown. Recently, Minoda et al. (2010) showed that the red alga *Cyanidioschyzon merolae* increased *rbcL* transcription at high levels of NADPH, 3-phoshoglyceric acid (3-PGA), or ribulose-1,5-bisphosphate (RuBP) under the influence of the transcription factor Ycf30. In addition, it has been reported that regeneration of RuBP could be a limiting factor for the CBB cycle in high CO_2 conditions (von Caemmerer and Farquhar, 1981; Stitt, 1991; Onoda et al., 2005). Thus, one possible mechanism underlying the reduction of diatom *rbcL* transcription observed in our study is related to a decrease in RuBP concentration in the chloroplasts due to the increase in CO_2 availability for diatoms. Because diatoms possess the same type of RubisCO (Form ID) and gene homologs encoding the Ycf30 protein (i.e., *ycf30*) (Kowallik et al., 1995), they could control *rbcL* gene expression using the same mechanisms as *C. merolae*. Further studies using marine diatom cultures are required to obtain a better understanding of the physiological mechanisms controlling the expression of RubisCO.

In our experiment, the rarefaction curves plateaued to some extent in all treatments (Fig. 5), indicating that the clone numbers screened from each library were statistically

sufficient for further diversity analysis. Taxonomic compositions in the cDNA library were considerably different from those in the diatom carbon biomass revealed by microscopic analysis by Sugie et al. (2013), which were composed primarily by Chaetocerataceae. This implies that the predominant diatoms did not necessarily become transcriptionally active *rbcL* phylotypes in our experiment. In addition, because 16–42% of the sequences were classified as unidentified diatoms or other eukaryotes, the primer set used in this study might be insufficient to estimate diatom composition at the family level.

The *rbcL* cDNA libraries in the Fe-added treatments differed significantly from the initial library, whereas those in the control treatments were not significantly different (Table 3), suggesting that the diatom blooms induced by Fe infusion were associated with the change in the relative contribution of *rbcL* expression in diatoms. For example, compared to the initial seawater, the relative contributions of Chaetocerataceae and unidentified centrics to the *rbcL* cDNA library increased markedly in the Fe-added bottles whereas they remained minor components in the control bottles (Fig. 6). This indicates that the relative significance of the RubisCO activity of these phylotypes could be increased by Fe enrichment. In addition, cDNA libraries were significantly different from each other at different CO_2 levels in the Fe-added bottles (Table 3). This indicates that the transcriptionally active phylotypes in diatoms could shift in response to an increase in the CO_2 level. On the other hand, the diversity indices for the diatom-specific *rbcL* cDNA sequences were not affected by CO_2 availability (Table 2). In addition, the highest chao1 (richness) value was observed in C-600 treatment. These results suggest that the richness and/or diversity of diatom phylotypes actively transcribing *rbcL* gene could remain under elevated CO_2 levels.

5 Conclusion

The present study showed that an increase in CO_2 levels could have negative impacts on diatom biomass in the Bering Sea, especially under Fe-limited conditions. Because diatoms play pivotal roles in carbon sequestration and food webs in the Bering Sea (Springer et al., 1996; Takahashi et al., 2002), our results indicate that ocean acidification might alter the biogeochemical processes and ecological dynamics in the

563 study area. Although the present results cannot be extrapolated to other HNLC
564 ecosystems due to differences in other environmental conditions, our findings suggest
565 that the combined effects of CO_2 and other environmental factors such as Fe availability
566 need to be examined for a better understanding of the potential impacts of ocean
567 acidification on marine ecosystems.

568 We examined, for the first time, the relationships between CO_2 levels or Fe
569 availability and RubisCO expression of diatoms in the Bering Sea. Significant decreases
570 in the *rbcL* expression of diatoms were observed at elevated CO_2 levels in both the
571 Fe-limited and Fe-enriched treatments, suggesting that ocean acidification could reduce
572 the primary productivity in the study area. Our results indicate that the amount of *rbcL*
573 transcripts could be an important indicator to assess the physiological responses of
574 RubisCO activity in diatoms to environmental drivers. However, photosynthetic carbon
575 fixation in diatoms can be controlled not only by RubisCO activity, but also other
576 processes such as carbon concentrating mechanisms (CCMs) and/or RuBP regeneration
577 (Rost et al., 2003; Onoda et al., 2005). More detailed studies on molecular mechanisms
578 are required to clarify the physiological responses of the diatom community to CO_2 and
579 Fe availability.

580

581 **6 Acknowledgements**

582 We thank the captain, officers, and crew of the R/V *Hakuho Maru* for their great
583 support and field assistance. We also thank J. Nishioka for Fe analysis. We also
584 appreciate the editor and three referees for providing constructive comments on the
585 manuscripts. This work was conducted within the framework of the Plankton
586 Ecosystem Response to CO_2 Manipulation Study (PERCOM) and was partly supported
587 by the grants from CRIEPI (#090313) and Grant-in-Aid for Scientific Research
588 (#18067008, #22681004).

589

590 **7 References**

591 Badger, M. R., Whitney, S. M., Ludwig, M., Yellowlees, D. C., Leggat, W., and Price,
592 G. D.: The diversity and co-evolution of RubisCO, plastids, pyrenoids, and
593 chloroplast based CO_2-concentrating mechanisms in algae, Can. J. Bot., 76, 1052–

1071, 1998.

Banse, K., and English, D. C.: Comparing phytoplankton seasonality in the eastern and western subarctic Pacific and the western Bering Sea, Prog. Oceanogr., 43, 235–288, 1999.

Boelen, P., van de Poll, W. H., van de Strate, H. J, Neven, I. A., Beardall, J., Buma, A. G. J.: Neither elevated nor reduced CO_2 affects the photophysiological performance of the marine Antarctic diatom *Chaetoceros brevis*, J. Exp. Mar. Biol. Ecol., 406, 38–45, 2011.

Caldeira, K., and Wickett, M. E.: Anthropogenic carbon and ocean pH. Nature, 425, 365, 2003.

Chao, A.: Nonparametric estimation of the number of classes in a population. Scand. J. Stat., 265–270, 1984.

Collins, S., Rost, B., and Rynearson, T. A.: Evolutionary potential of marine phytoplankton under ocean acidification, Evol. Appl., 7, 140–155, 2014.

Corredor, J. E., Wawrik, B., Paul, J. H., Tran, H., Kerkhof, L., Lopez, J. M, Dieppa, A., and Cardenas, O.: Geochemical rate-RNA integrated study: ribulose-1,5-bisphosphate carboxylase/oxygenase gene transcription and photosynthetic capacity of planktonic photoautotrophs, Appl. Environ. Microbiol., 70, 5459–5468, 2004.

Curtis, P. S., Drake, B. G., and Whigham, D. F.: Nitrogen and carbon dynamics in C_3 and C_4 marsh plants grown under elevated CO_2 in situ, Oecologia, 78, 297–301, 1989.

Edmond, J. M.: High precision determination of titration alkalinity and total carbon dioxide content of sea water by potentiometric titration, Deep-Sea Res., 17, 737–750, 1970.

Endo, H., Yoshimura, T., Kataoka, T., and Suzuki, K.: Effects of CO_2 and iron availability on phytoplankton and eubacterial community compositions in the northwest subarctic Pacific, J. Exp. Mar. Biol. Ecol., 439, 160–175, 2013.

Engel, A., Schulz, K. G., Riebesell, U., Bellerby, R., Delille, B., Schartau, M.: Effects of CO_2 on particle size distribution and phytoplankton abundance during a mesocosm bloom experiment (PeECE II), Biogeosciences, 5, 509–521, 2008.

Feng, Y., Hare, C. E., Leblanc, K., Rose, J. M., Zhang, Y., DiTullio, G. R., Lee, P. A., Wilhelm, S. W., Rowe, J. M., Sun, J., Nemcek, N., Gueguen, C., Passow, U., Benner, I., Brown, C., and Hutchins, D. A.: Effects of increased pCO_2 and temperature on the North Atlantic spring bloom. I. The phytoplankton community and biogeochemical response, Mar. Ecol. Prog. Ser. 388, 13–25, 2009.

Feng, Y., Hare, C. E., Rose, J. M., Handy, S. M., DiTullio, G. R., Lee, P. A., Smith Jr, W. O., Peloquin, J., Tozzi, S., Sun, J., Zhang, Y., Dunbar, R. B., Long, M. C., Sohst, B., Lohan, M., and Hutchins, D. A.: Interactive effects of iron, irradiance

633 and CO_2 on Ross Sea phytoplankton, Deep-Sea Res. I, 57, 368–383, 2010.

634 Gontero, B., and Salvucci, M. E.: Regulation of photosynthetic carbon metabolism in
635 aquatic and terrestrial organisms by Rubisco activase, redox-modulation and
636 CP12, Aquat. Bot., 118, 14–23, 2014.

637 Granum, E., Roberts, K., Raven, J. A., Leegood, R. C.: Primary carbon and nitrogen
638 metabolic gene expression in the diatom *Thalassiosira pseudonana*
639 (Bacillariophyceae): Diel periodicity and effects of inorganic carbon and nitrogen,
640 J. Phycol., 45, 1083–1092, 2009.

641 Hare, C. E., Leblanc, K., DiTullio, G. R., Kudela, R. M., Zhang, Y., Lee, P. A.,
642 Riseman, S., and Hutchins, D. A.: Consequences of increased temperature and
643 CO_2 for phytoplankton community structure in the Bering Sea, Mar. Ecol. Prog.
644 Ser., 352, 9–16, 2007.

645 Harrison, P.J., Conway, H.L., Holmes, R.W., and Davis, C.O.: Marine diatoms grown
646 in chemostats under silicate or ammonium limitation. III. Cellular chemical
647 composition and morphology of *Chaetoceros debilis*, *Skeletonema costatum*, and
648 *Thalassiosira gravida*, Mar. Biol., 43(1), 19–31, 1977.

649 Hoppe, C. J., Hassler, C. S., Payne, C. D., Tortell, P. D., Rost, B. and Trimborn, S.: Iron
650 limitation modulates ocean acidification effects on Southern Ocean phytoplankton
651 communities, PloS One, 8(11), e79890, 2013.

652 Ihnken, S., Roberts, S., and Beardall, J.: Differential responses of growth and
653 photosynthesis in the marine diatom *Chaetoceros muelleri* to CO_2 and light
654 availability, Phycologia, 50, 182–193, 2011.

655 Jeffrey, S.W., and Wright, S.W.: Photosynthetic pigments in the Haptophyta, in: The
656 Haptophyte algae, Green, J. C., and Leadbeater, B. S. C. (Eds.), Carendon Press,
657 Oxford, 111–132, 1994.

658 Jiang, Y., Yin, K., Berges, J.A., and Harrison, P.J.: Effects of silicate resupply to
659 silicate-deprived *Thalassiosira weissflogii* (Bacillariophyceae) in stationary or
660 senescent phase: short-term patterns of growth and cell death, J. Phycol., 50(3),
661 602–606, 2014

662 John, D. E., Jose, López-Díaz, J. M., Cabrera, A., Santiago, N. A., Corredor, J. E.,
663 Bronk, D. A., and Paul, J. H.: A day in the life in the dynamic marine
664 environment: how nutrients shape diel patterns of phytoplankton photosynthesis
665 and carbon fixation gene expression in the Mississippi and Orinoco River plumes,
666 Hydrobiologia, 679, 155–173, 2010.

667 John, D. E., Patterson, S. S., and Paul, J. H.: Phytoplankton group specific quantitative
668 polymerase chain reaction assays for RuBisCO mRNA transcripts in seawater,
669 Mar. Biotechnol., 9, 747–759, 2007a.

670 John, D. E., Wang, Z. A., Liu, X. W., Byrne, R. H., Corredor, J. E., Lopez, J. M.,
671 Cabrera, A., Bronk, D. A., Tabita, F. R., and Paul, J. H.: Phytoplankton carbon
672 fixation gene (RuBisCO) transcripts and air-sea CO_2 flux in the Mississippi River

673 plume, ISME J., 1, 517–531, 2007b.

674 Kim, J. -M., Lee, K., Shin, K., Kang, J. -H., Lee, H. -W., Kim, M., Jang, P. -G., and
675 Jang, M. -C.: The effect of seawater CO_2 concentration on growth of the natural
676 phytoplankton assemblage in a controlled mesocosm experiment, Limnol.
677 Oceanogr., 51, 1629–1636, 2006.

678 Kowallik, K. V., Stoebe, B., Schaffran, I., KrothPancic, P., and Freier, U.: The
679 chloroplast genome of a chlorophyll *a*+*c*-containing alga, Odontella sinensis,
680 Plant Mol. Biol. Rep., 13, 336–342, 1995.

681 Latasa, M.: Improving estimations of phytoplankton class abundances using
682 CHEMTAX, Mar. Ecol. Progr. Ser., 329, 13–21, 2007.

683 Lewis, E., and Wallance, D. W. R.: Program developed for CO_2 system calculations.
684 ORNL/CDIAC-105. Carbon dioxide information analysis center, Oak Ridge
685 National Laboratory, US Department of Energy, Oak Ridge, Tennessee, 1998.

686 Losh, J. L., Morel, F. M. M., and Hopkinson, B. M.: Modest increase in the C:N ratio of
687 N-limited phytoplankton in the California Current in response to high CO_2, Mar.
688 Ecol. Prog. Ser., 468, 31–42, 2012.

689 Losh, J. L., Young, J. N., and Morel, F. M.: Rubisco is a small fraction of total protein
690 in marine phytoplankton, New Phytol., 198, 52–58, 2013.

691 Luu-The, V., Paquet, N., Calvo, E., and Cumps, J.: Improved real-time RT-PCR method
692 for high-throughput measurements using second derivative calculation and double
693 correction, Biotechniques, 38, 287–293, 2005.

694 Mackey, M. D., Mackey, D. J., Higgins, H. W., and Wright, S. W.: CHEMTAX-a
695 program for estimating class abundances from chemical markers: application to
696 HPLC measurements of phytoplankton, Mar. Ecol. Progr. Ser., 144, 265–283,
697 1996.

698 Mackinder, L., Wheeler, G., Schroeder, D., Riebesell, U., and Brownlee, C.: Molecular
699 mechanisms underlying calcification in coccolithophores, Geomicrobiology, 27,
700 585–595, 2010.

701 Makino, A., Sakuma, H., Sudo, E., and Mae, T.: Differences between Maize and Rice in
702 N-use efficiency for photosynthesis and protein allocation, Plant Cell Physiol., 44,
703 952–956, 2003.

704 Matsuda, Y., Nakajima, K., and Tachibana, M.: Recent progresses on the genetic basis
705 of the regulation of CO_2 acquisition systems in response to CO_2 concentration,
706 Photosynth. Res., 109, 191–203, 2011.

707 Meakin, N. G., and Wyman, M.: Rapid shifts in picoeukaryote community structure in
708 response to ocean acidification, ISME J., 5, 1397–1405, 2011.

709 Meehl, G. A., Stocker, T. F., Collins, W. D., Friedlingsten, P., Gaye, A. T., Gregory, J.
710 M., Kitoh, A., Knutti, R., Murphy, J. M., Noda, A., Raper, S. C. B., Watterson, I.

711 G., Weaver, A. J., and Zhao, Z. -C.: Global Climate Projections, in: Climate
712 Change 2007 The Physical Science Basis, Contribution of Working Group I to the
713 Fourth Assessment Report of the Intergovernmental Panel on Climate Change,
714 Solomon, S., Qin, D., Manning, M., Chen, Z., Marquis, M., Averyt, K., Tignor, M.
715 M. B., and Miller, H.L (EDs.), Cambridge University Press, United Kingdom and
716 New York, 2007.

717 Michaels, A. F., and Silver, M. W.: Primary Production, sinking fluxes and the
718 microbial food web, Deep-Sea Res. 35, 473–490, 1988.

719 Minoda, A., Weber, A. P. M., Tanaka, K., and Miyagishima, S.: Nucleus-independent
720 control of the Rubisco operon by the plastid-encoded transcription factor Ycf30 in
721 the red alga *Cyanidioschyzon merolae*, Plant Physiol., 154, 1532–1540, 2010.

722 Obata, H., Karatani, H., and Nakayama, E.: Automated determination of iron in
723 seawater by chelating resin concentration and chemiluminescence detection, Anal.
724 Chem., 65, 1524–1528, 1993.

725 Ondrusek, M. E., Bidigare, R. R., Sweet, S. T, Defreitas, D. A., and Brooks, J. M.:
726 Distribution of phytoplankton pigments in the North Pacific Ocean in relation to
727 physical and optical variability, Deep-Sea Res., 38, 243-266, 1991.

728 Onoda, Y., Hikosaka, K., and Hirose, T.: Seasonal change in the balance between
729 capacities of RuBP carboxylation and RuBP regeneration affects CO_2 response of
730 photosynthesis in *Polygonum cuspidatum*, J. Exp. Bot., 56, 755–763, 2005.

731 Pearson, P. N., and Palmer, M. R.: Atmospheric carbon dioxide concentration over the
732 past 60 million years, Nature, 406, 659–699, 2000.

733 Pichard, S. L., Campbell, L., Kang, J. B., Tabita, F. R., and Paul, J. H.: Regulation of
734 ribulose bisphosphate carboxylase gene expression in natural phytoplankton
735 communities 1. Diel rhythms, Mar. Ecol. Progr. Ser., 139, 257–265, 1996.

736 Raven, J., Caldeira, K., Elderfield, H., Hoegh-Guldberg, O., Liss, P., Riebesell, U.,
737 Shepherd, J., Turley, C., and Watson, A.: Ocean acidification due to increasing
738 atmospheric carbon dioxide, The Royal Society policy document 12/05, Cardiff:
739 Clyvedon Press, 2005.

740 Riebesell, U., Schulz, K. G., Bellerby, R. G. J., Botros, M., Fritsche, P., Meyerhöfer, M.,
741 Neill, C., Nondal, G., Oschlies, A., Wohlers, J., and Zöllner, E.: Enhanced
742 biological carbon consumption in a high CO_2 ocean, Nature, 450 (7169), 545–548,
743 2007.

744 Riebesell, U., and Tortell, P. D.: Effects of ocean acidification on pelagic organisms and
745 ecosystems, in: Ocean acidification, Gattuso, J.-P., and Hansson, L. (Eds.),
746 Oxford University Press, New York, 83–98, 2011.

747 Rost, B., Riebesell, U., Burkhardt, S., and Sültemeyer, D.: Carbon acquisition of bloom
748 forming marine phytoplankton, Limnol. Oceanogr. 48, 55–67, 2003.

749 Sabine, C. L., Feely, R. A., Gruber, N., Key, R. M., Lee, K., Bullister, J.L., Wanninkhof,
750 R., Wong, C. S., Wallace, D. W. R., Tilbrook, B., Millero, F. J., Peng, T. -H.,
751 Kozyr, A., Ono, T., and Rios, A. F.: The oceanic sink for anthropogenic CO_2,
752 Science, 305, 367–371, 2004.

753 Schloss, P. D., Westcott, S. L., Ryabin, T., Hall, J. R., Hartmann, M., Hollister, E. B.,
754 Lesniewski, R. A., Oakley, B. B., Parks, D. H., Robinson, C. J., Sahl, J. W., Stres,
755 B., Thallinger, G. G., Van Horn, D. J., and Weber, C. F.: Introducing mothur:
756 open-source, platform-independent, community-supported software for describing
757 and comparing microbial communities, Appl. Environ. Microbiol., 75, 7537–7541,
758 2009.

759 Schoemann, V., Becquevort, S., Stefels, J., Rousseau, V., and Lancelot, C.: Phaeocystis
760 blooms in the global ocean and their controlling mechanisms: a review, J. Sea
761 Res., 53, 43−66, 2005.

762 Shannon, C. E.: A mathematical theory of communication, AT&T Teck. J., 27, 379–423,
763 1948.

764 Shi, D., Xu, Y., Hopkinson, B. M., Morel, F. M. M.: Effect of ocean acidification on
765 iron availability to marine phytoplankton, Science, 327, 676–679, 2010.

766 Simpson, E. H.: Measurement of diversity, Nature, 163, 688, 1949.

767 Singleton, D. R., Furlong, M. A., Rathbun, S. L., and Whitman, W. B.: Quantitative
768 comparisons of 16S rRNA gene sequence libraries from environmental samples,
769 Appl. Environ. Microbiol., 67, 4374–4376, 2001.

770 Smith, C. J., Nedwell, D. B., Dong, L. F., and Osborn, A. M.: Evaluation of quantitative
771 polymerase chain reaction-based approaches for determining gene copy and gene
772 transcript number in environmental samples, Environ. Microbiol., 8, 804–815,
773 2006.

774 Springer, A. M., McRoy, C. P., and Flint, M. V.: The Bering Sea Green Belt: shelf-edge
775 processes and ecosystem production, Fish. Oceanogr., 5, 205–223, 1996.

776 Stitt, M.: Rising CO_2 levels and their potential significance for carbon flow in
777 photosynthetic cells, Plant Cell Environ., 14, 741–762, 1991.

778 Sugie, K., Endo, H., Suzuki, K., Nishioka, J., Kiyosawa, H., and Yoshimura, T.:
779 Synergistic effects of pCO_2 and iron availability on nutrient consumption ratio of
780 the Bering Sea phytoplankton community, Biogeosciences, 10, 6309–6321, 2013.

781 Suzuki, K., Kuwata, A., Yoshie, N., Shibata, A., Kawanobe, K., and Saito, H.:
782 Population dynamics of phytoplankton, heterotrophic bacteria, and viruses during
783 the spring bloom in the western subarctic Pacific, Deep-Sea Res. I, 58, 575–589,
784 2011.

785 Suzuki, K., Minami, C., Liu, H., and Saino, T.: Temporal and spatial patterns of
786 chemotaxonomic algal pigments in the subarctic Pacific and the Bering Sea
787 during the early summer of 1999, Deep-Sea Res. II, 49, 5685–5704, 2002.

788 Takahashi, K., Fujitani, N., and Yanada, M.: Long term monitoring of particle fluxes in
789 the Bering Sea and the central subarctic Pacific Ocean, 1990–2000, Prog.
790 Oceanogr., 55. 95–112, 2002.

791 Tortell, P. D., DiTullio, G. R., Sigman, D. M., and Morel, F. M. M.: CO_2 effects on
792 taxonomic composition and nutrient utilization in an Equatorial Pacific
793 Phytoplankton assemblage, Mar. Ecol. Prog. Ser., 236, 37–43, 2002.

794 Tortell, P. D., Payne, C. D., Li, Y., Trimborn, S., Rost, B., Smith, W. O., Riesselan, C.,
795 Dunbar, R. B., Sedwick, P., and DiTullio, G. R.: CO_2 sensitivity of Southern
796 Ocean phytoplankton, Geophys. Res. Let., *35*(4), L04605, 2008.

797 Trimborn, S., Brenneis, T., Sweet, E., and Rost, B.: Sensitivity of Antarctic
798 phytoplankton species to ocean acidification: Growth, carbon acquisition, and
799 species interaction, Limnol. Oceanogr., 58, 997–1007, 2013.

800 Von Caemmerer, S. V., and Farquhar, G. D.: Some relationships between the
801 biochemistry of photosynthesis and the gas exchange of leaves, Planta, 153, 376–
802 387, 1981.

803 WMO.: Greenhouse gas bulletin: The state of greenhouse gases in the atmosphere based
804 on global observations through 2012. World Meteorological Organization,
805 Geneva, Switzerland, ISSN 2078–0796, 2013.

806 Wawrik, B., Paul, J. H., and Tabita, F. R.: Real-time PCR quantification of *rbcL*
807 (ribulose-1,5-bisphosphate carboxylase/oxygenase) mRNA in diatoms and
808 pelagophytes, Appl. Environ. Microbiol., 68, 3771–3779, 2002.

809 Welschmeyer, N. A.: Fluorometric analysis of chlorophyll *a* in the presence of
810 chlorophyll *b* and pheopigments, Limnol. Oceanogr., 39, 1985–1992, 1994.

811 Wright, S. W., and van den Enden, R. L.: Phytoplankton community structure and
812 stocks in the east Antarctic marginal ice zone (BROKE survey, January-March
813 1996) determined by CHEMTAX analysis of HPLC pigment signature, Deep-Sea
814 Res. II, 47, 2363–2400, 2000.

815 Xu, H. H., and Tabita, F. R.: Ribulose-1.5-bisphosphate carboxylase/oxygenase gene
816 expression and diversity of lake Erie planktonic microorganisms, Appl. Environ.
817 Microbiol, 62, 1913–1921, 1996.

818 Yoshimura, T., Nishioka, J., Suzuki, K., Hattori, H., Kiyosawa, H., Watanabe, Y.:
819 Impacts of elevated CO_2 on organic carbon dynamics in nutrient depleted Okhotsk
820 Sea surface waters, J. Exp. Mar. Biol. Ecol., 395, 191–198, 2010.

821 Yoshimura, T., Sugie, K., Endo, H., Suzuki, K., Nishioka, J., and Ono, T.: Organic
822 matter production response to CO_2 increase in open subarctic plankton
823 communities: Comparison of six microcosm experiments under iron-limited
824 and-enriched bloom conditions, Deep-Sea Res. I, 94, 1–14, 2014.

825 Yoshimura, T., Suzuki, K., Kiyosawa, H., Ono, T., Hattori, H., Kuma, K., and Nishioka,
826 J.: Impacts of elevated CO_2 on particulate and dissolved organic matter

827 production: Microcosm experiments using iron deficient plankton communities in
828 open subarctic waters, J. Oceanogr., 69, 601–618, 2013.

Table 1. Carbonate chemistry, nutrients, and Fe parameters (value ± 1 standard deviation, n = 3) during the incubation experiment. Carbonate parameters are the initial and mean values throughout the incubation. Macronutrients and Fe parameters are the values at the initial or final sampling days (i.e., day 5 for the control and day 6 for the Fe-added treatments). Standard deviation was not assessed for initial TD-Fe concentration because samples were collected from single source. See figures S1 and S2 for the complete data set.

	DIC ($\mu mol\ kg^{-1}$)	TA ($\mu mol\ kg^{-1}$)	pCO_2 (μatm)	CO_2 ($\mu mol\ kg^{-1}$)	pH (Total scale)
C-Initial	2086.4 ± 2.8	2249.1 ± 5.0	388.4 ± 18.1	18.4 ± 0.9	8.05 ± 0.02
C-380	2075.5 ± 8.1	2252.9 ± 10.8	355.7 ± 34.7	16.8 ± 1.6	8.09 ± 0.04
C-600	2151.6 ± 7.8	2250.9 ± 4.7	604.1 ± 36.2	28.5 ± 1.7	7.88 ± 0.02
Fe-Initial	2085.3 ± 0.8	2250.0 ± 4.9	383.4 ± 12.6	18.1 ± 0.6	8.06 ± 0.01
Fe-180	1959.9 ± 62.0	2244.1 ± 16.0	202.0 ± 50.9	9.5 ± 2.4	8.21 ± 0.10
Fe-380	2068.5 ± 27.7	2235.7 ± 14.9	375.9 ± 47.9	17.8 ± 2.3	8.01 ± 0.05
Fe-600	2120.6 ± 33.5	2248.5 ± 12.0	512.6 ± 135.5	24.2 ± 6.4	7.96 ± 0.11
Fe-1000	2200.2 ± 12.6	2248.4 ± 9.8	913.8 ± 159.8	43.2 ± 7.6	7.72 ± 0.07

Table 1. (Continued)

	Nitrate ($\mu mol\ L^{-1}$)	Phosphate ($\mu mol\ L^{-1}$)	Silicic acid ($\mu mol\ L^{-1}$)	TD-Fe ($nmol\ L^{-1}$)
C-Initial	18.06 ± 0.10	1.47 ± 0.01	16.95 ± 0.12	1.35
C-380	7.09 ± 0.27	0.65 ± 0.02	0.28 ± 0.05	0.27 ± 0.03
C-600	12.01 ± 0.27	0.98 ± 0.02	3.04 ± 0.32	0.29 ± 0.04
Fe-Initial	18.09 ± 0.11	1.47 ± 0.01	16.90 ± 0.12	5.50 ± 0.10
Fe-180	0.13 ± 0.04	0.10 ± 0.01	0.66 ± 0.09	4.60 ± 0.19
Fe-380	0.09 ± 0.00	0.12 ± 0.04	0.50 ± 0.01	4.48 ± 0.12
Fe-600	0.08 ± 0.00	0.10 ± 0.00	0.50 ± 0.01	4.34 ± 0.08
Fe-1000	0.08 ± 0.00	0.08 ± 0.02	0.47 ± 0.02	4.18 ± 0.24

841 **Table 2.** Number of OTUs, richness index, and diversity indices (value ± 95%
842 confidence interval) for *rbcL* cDNA libraries obtained from the initial seawater and the
843 incubation bottles on day 2 (Fe-380 and Fe-600) and day 3 (C-380 and C-600).
844

Library	No. of sequences	No. of OTUs	Chao1	*H'*	1−*D*
Initial	35	10	25.0	1.81 ± 0.32	0.197 ± 0.086
C-380	50	15	20.0	1.98 ± 0.36	0.232 ± 0.110
C-600	50	14	29.0	1.60 ± 0.41	0.369 ± 0.148
Fe-380	50	13	23.0	2.24 ± 0.23	0.116 ± 0.042
Fe-600	50	12	19.5	2.01 ± 0.26	0.158 ± 0.053

845

Table 3. Significance levels for differences among *rbcL* cDNA libraries as calculated with LIBSHUFF. p values < 0.05 are bolded.

	Library (Y)				
	Initial	C-380	C-600	Fe-380	Fe-600
Library (X)					
Initial	—	0.434	0.573	0.383	0.587
C-380	0.153	—	0.086	0.101	0.898
C-600	0.523	0.500	—	**0.004**	0.033
Fe-380	**<0.001**	**<0.001**	**<0.001**	—	**0.002**
Fe-600	**0.009**	**0.004**	**<0.001**	0.030	—

Figure captions

Figure 1. Temporal changes in fucoxanthin (a and b) and 19'-hexanoyloxyfucoxanthin (c and d) concentrations. Left (a and c) and right graphs indicate data from the control and Fe-added treatments, respectively. Error bars denote ± 1 standard deviation (SD, n = 3). Standard deviations were not assessed on days 2 (Fe-added treatmets) and 3 (control treatments) because samples were collected from each single bottle.

Figure 2. Mean contributions of each phytoplankton group to total Chl *a* biomass estimated by CHEMTAX in the (A) control bottles at 380 and 600 ppm CO_2, and (B) Fe-added bottles at 180, 380, 600 and 1000 ppm CO_2 (n = 1 or 3).

Figure 3. Relationship between fucoxanthin concentration and diatom-specific *rbcL* copy number ($y = 7.62\times10^{8}x+1.90\times10^{8}$, $r^2 = 0.677$, $p < 0.001$, n = 28).

Figure 4. Abundances of *rbcL* mRNA (cDNA) normalized to *rbcL* gene copy number (*rbcL* cDNA/DNA) in the control bottles on day 3 and the Fe-added bottles on day 2. Open bars and closed bars denote control and Fe-added treatments, respectively. Error bars indicate ± 1 SD (n = 3).

Figure 5. Rarefaction analysis of the diatom-specific *rbcL* clone libraries. The rarefaction curves, plotting the number of operational taxonomic units (OTUs) as a function of the number of sequences, were computed by the software mothur. C and Fe indicate the control and Fe-added treatments, respectively.

Figure 6. Relative phylotype contributions in the *rbcL* cDNA libraries obtained from the initial seawater and the incubation bottles at day 2 (Fe-380 and Fe-600) and day 3 (C-380 and C-600).

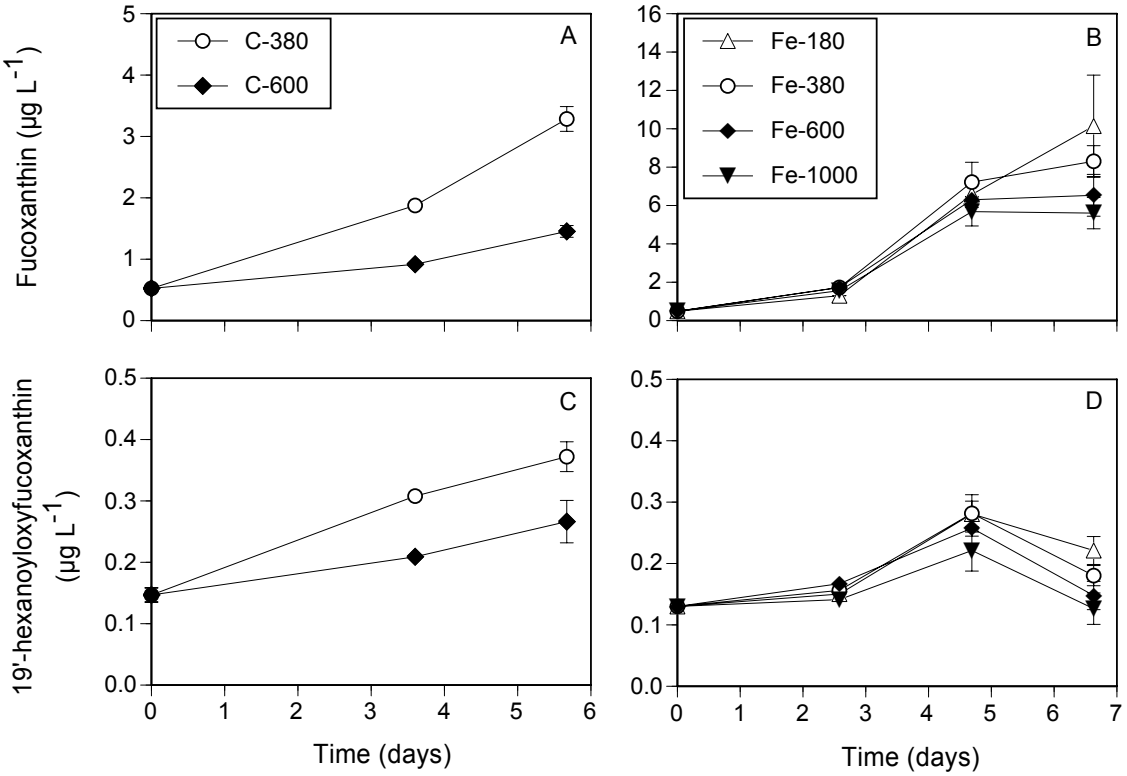

881

882 **Figure 1**

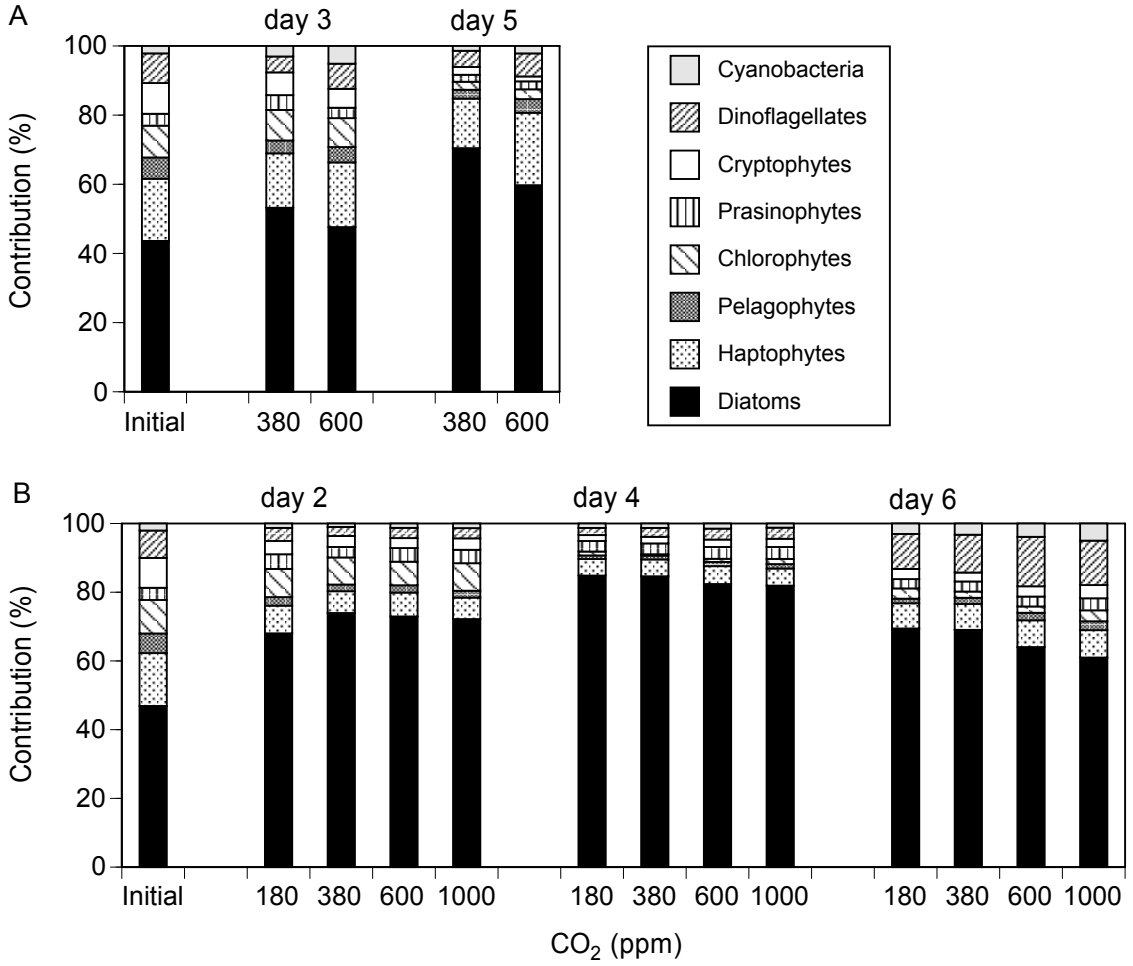

883

884 **Figure 2**

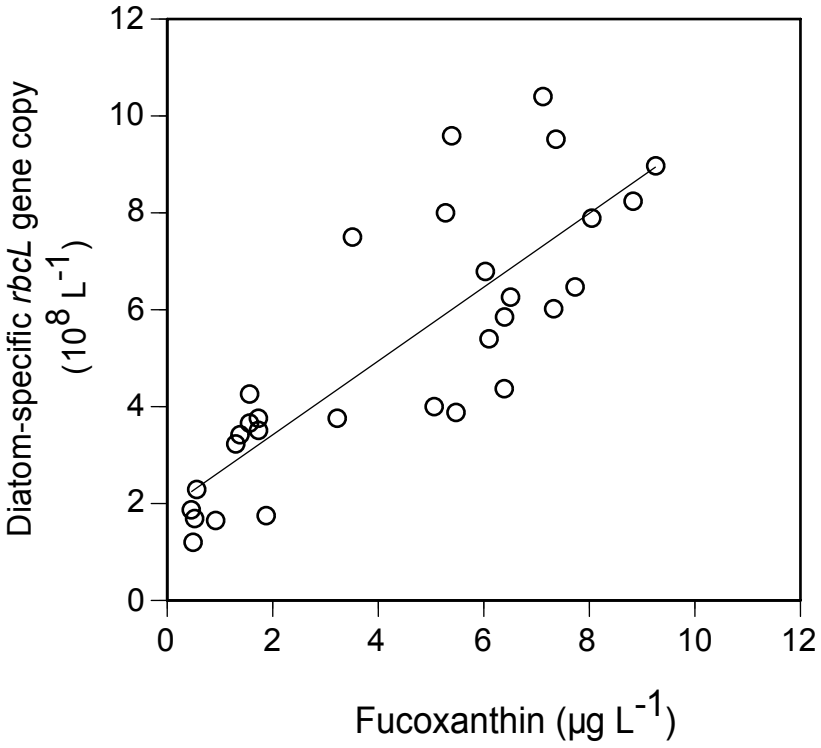

885

886 **Figure 3**

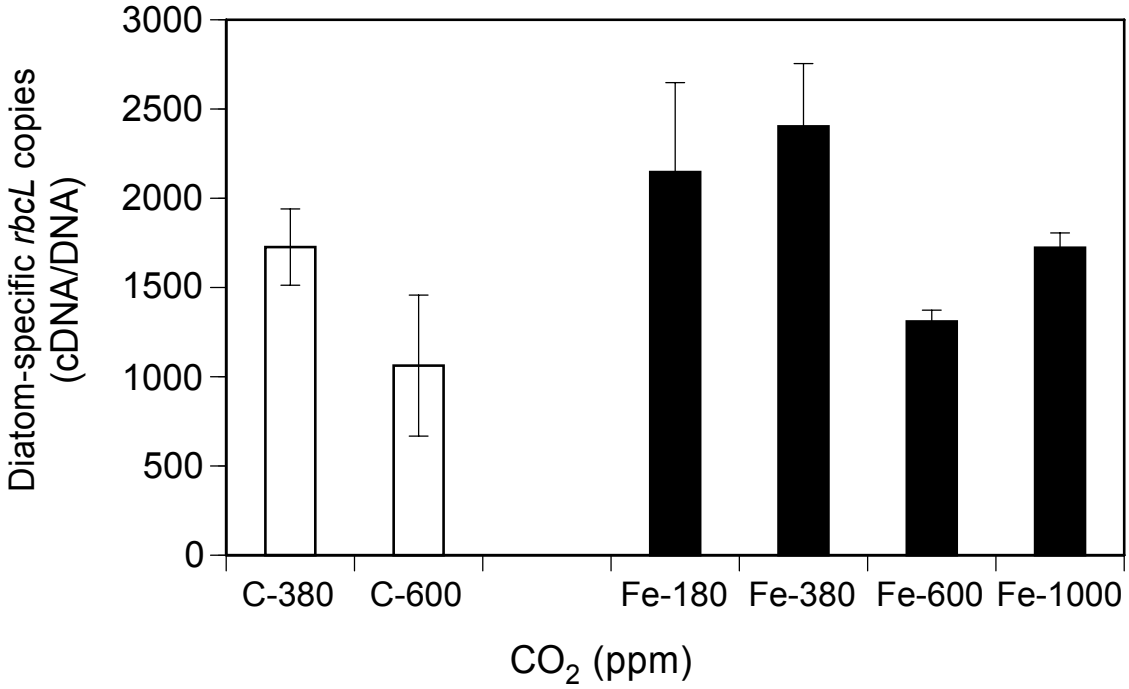

887

888 **Figure 4**

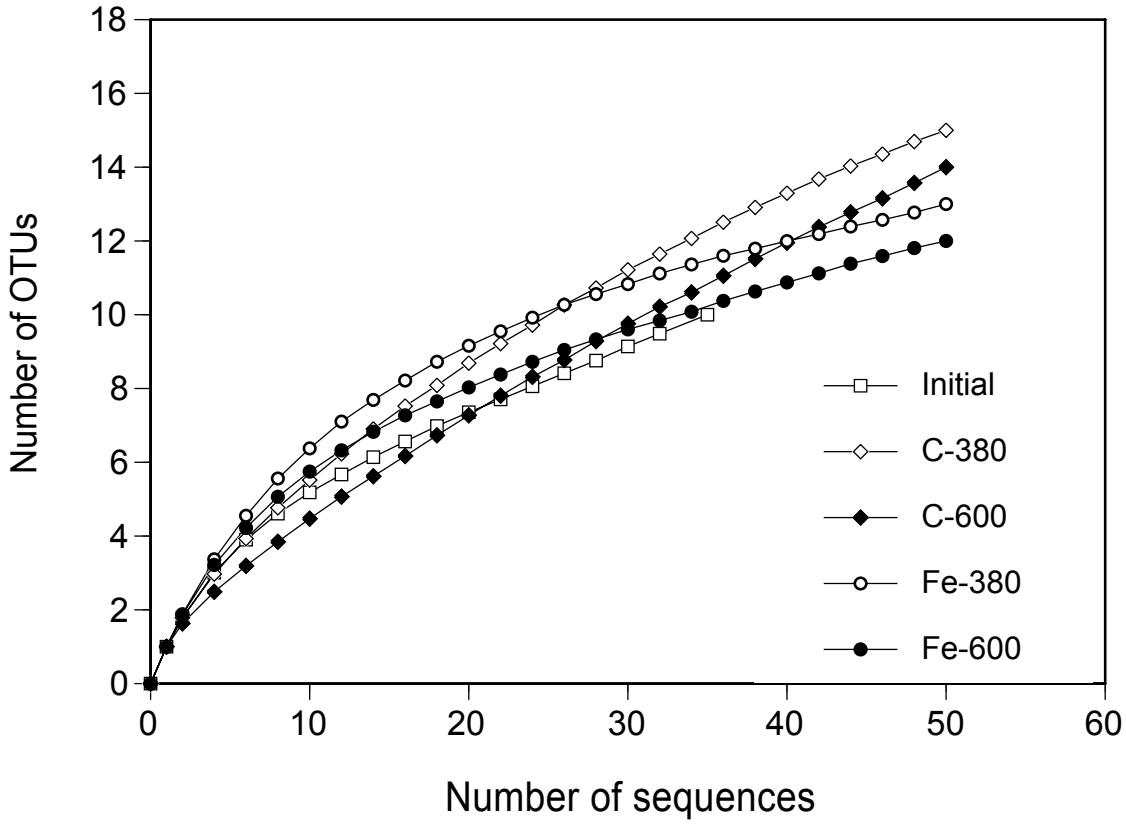

889

890 **Figure 5**

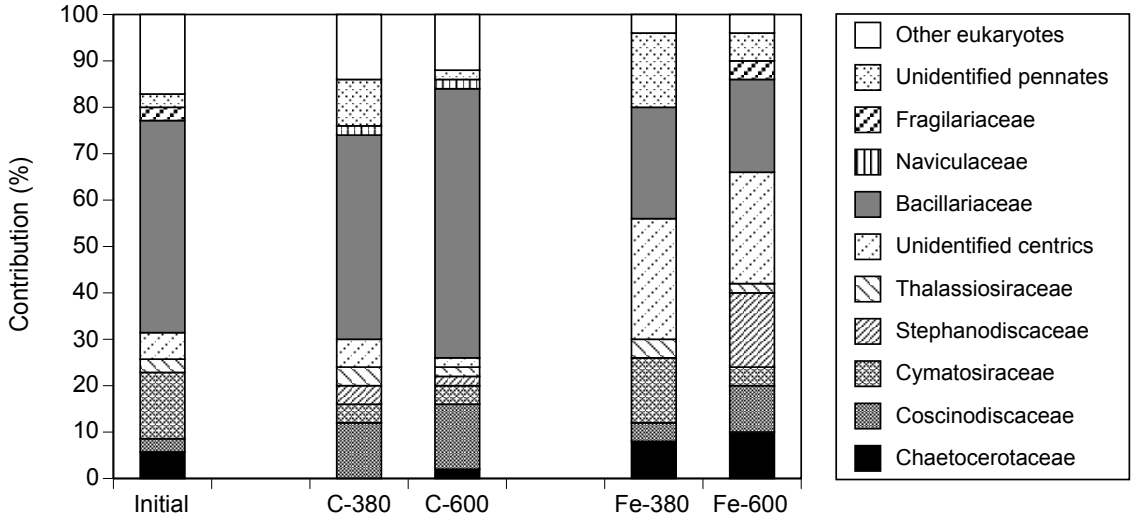

891

892 **Figure 6**